Supporting information for

$BaCe_{0.16}Y_{0.04}Fe_{0.8}O_{3-\delta}$ nanocomposite: A new high-performance cobalt-free triple-conducting cathode for protonic ceramic fuel cells operating at reduced temperatures

Dan Zou[1], Yongning Yi[1], Yufei Song[2], Daqin Guan[1], Meigui Xu[1], Ran Ran[1], Wei Wang[1*], Wei Zhou[1], Zongping Shao[1,3*]

[1] *State Key Laboratory of Materials-Oriented Chemical Engineering, College of Chemical Engineering, Nanjing Tech University, Nanjing 210009, China*

[2] *Department of Mechanical and Aerospace Engineering, The Hong Kong University of Science and Technology, Clear Water Bay, Hong Kong, China*

[3] *WA School of Mines: Minerals, Energy and Chemical Engineering (WASM-MECE), Curtin University, Perth, WA 6845, Australia*

*** Corresponding authors**

E-mail: wangwei@njtech.edu.cn (W. Wang); shaozp@njtech.edu.cn (Z. Shao)

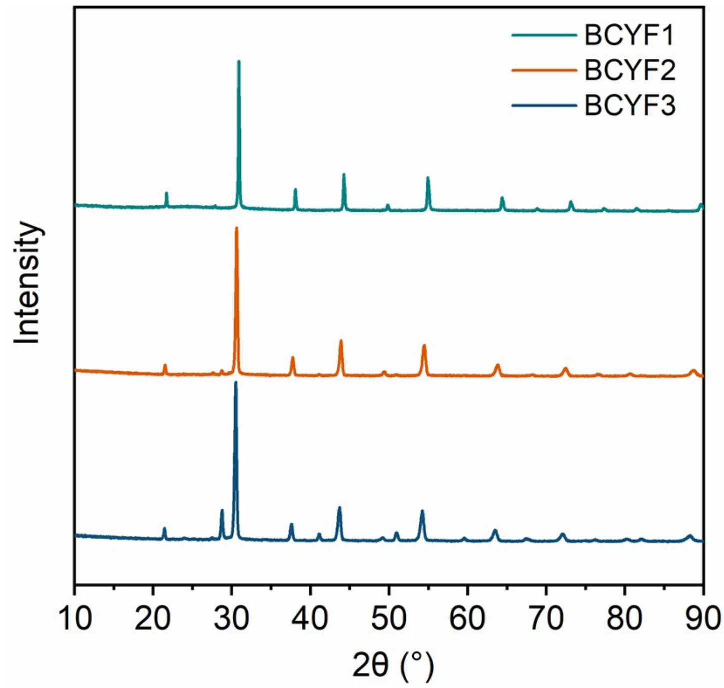

Fig. S1. XRD patterns of as-synthesized BCYF1, BCYF2 and BCYF3 samples after a natural cooling from 1000 °C to room temperature.

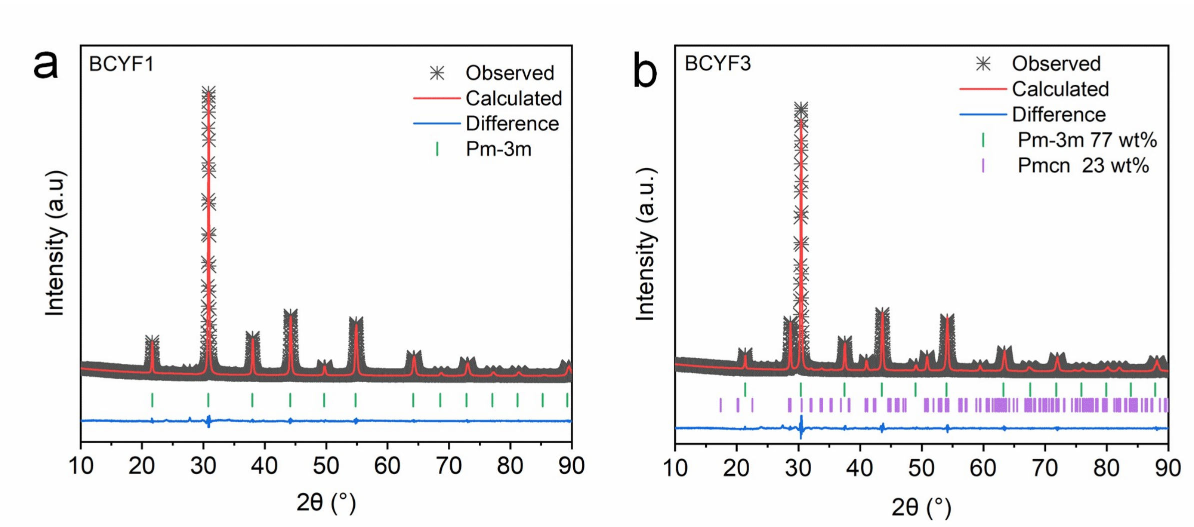

Fig. S2. Refined XRD patterns of (a) BCYF1 and (b) BCYF3.

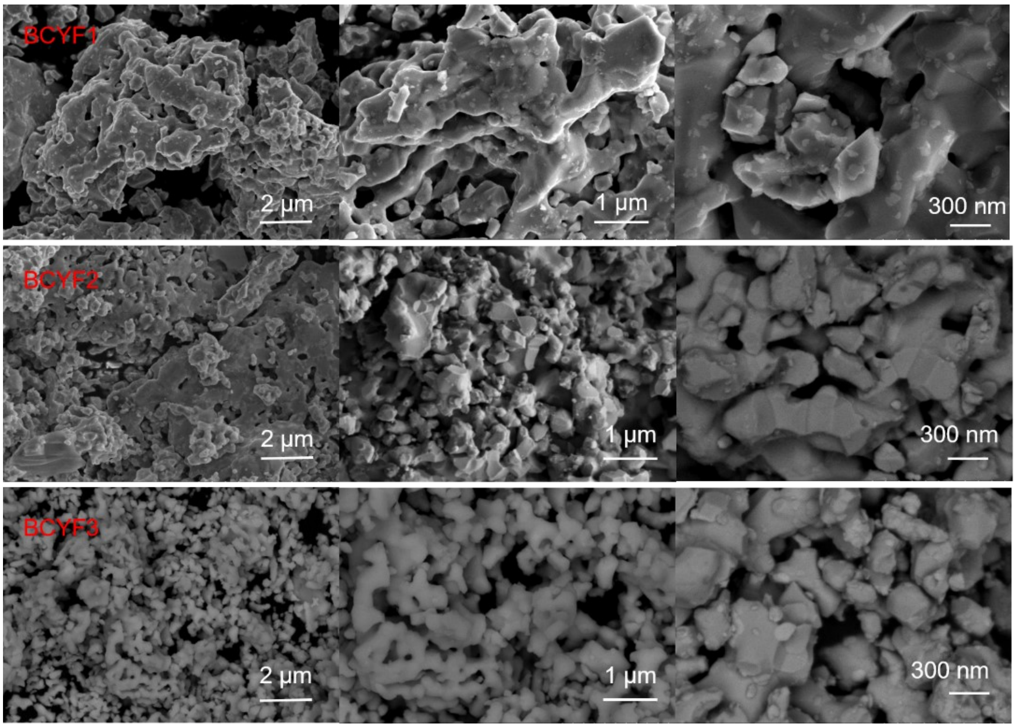

Fig. S3. SEM images of BCYF1, BCYF2 and BCYF3 samples.

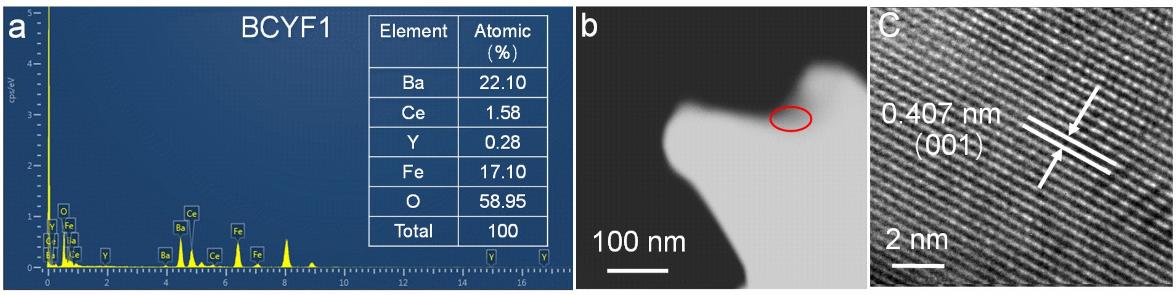

Fig. S4. (a) Point EDX scanning results, (b) STEM image, (c) HR-TEM image of BCYF1.

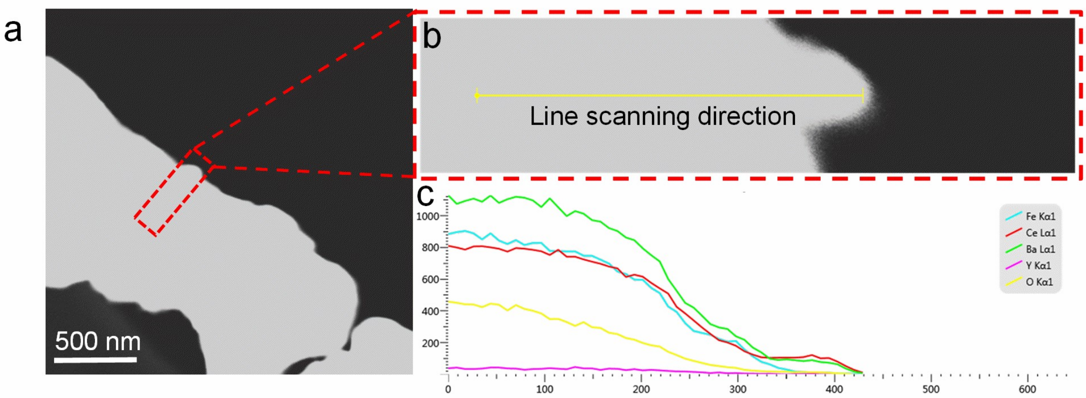

Fig. S5. Linear EDX scanning results of BCYF2: (a) STEM image, (b) line scanning area selected from Fig. S4, (c) linear EDX scanning results.

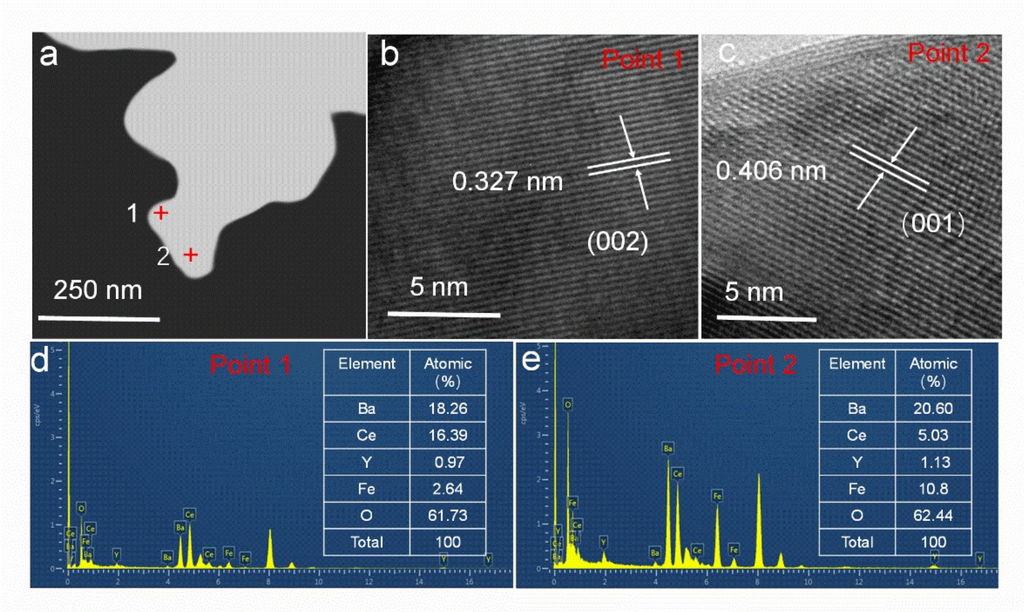

Fig. S6. (a) STEM image, (b, c) HR-TEM images of point 1 and 2 and (d, e) point EDX scanning results of BCYF3.

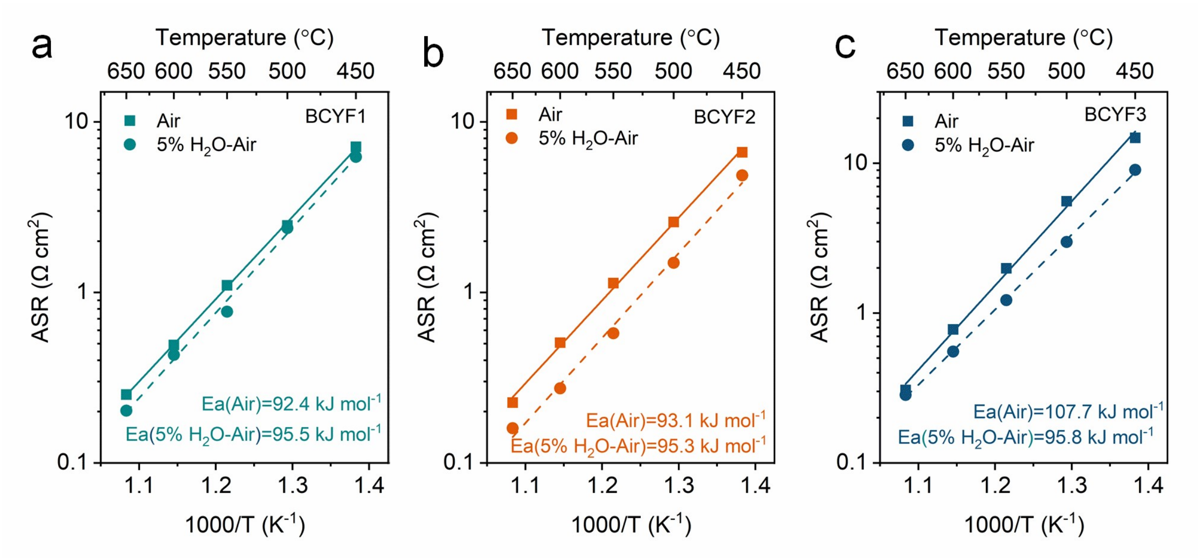

Fig. S7. Arrhenius plots of ASR values of various cathodes in BZCYYb-supported symmetrical cells in air and in 5 vol.% H_2O-air: (a) BCYF1, (b) BCYF2 and (c) BCYF3.

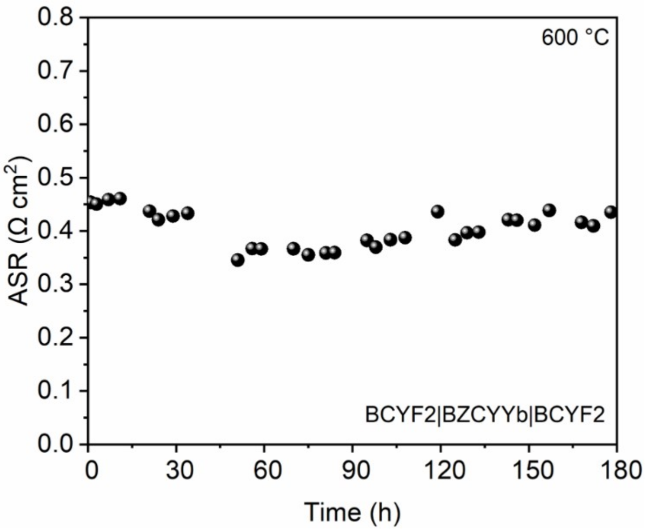

Fig. S8. ASR stability of BCYF2 cathode in a symmetrical cell at 600 °C in wet air.

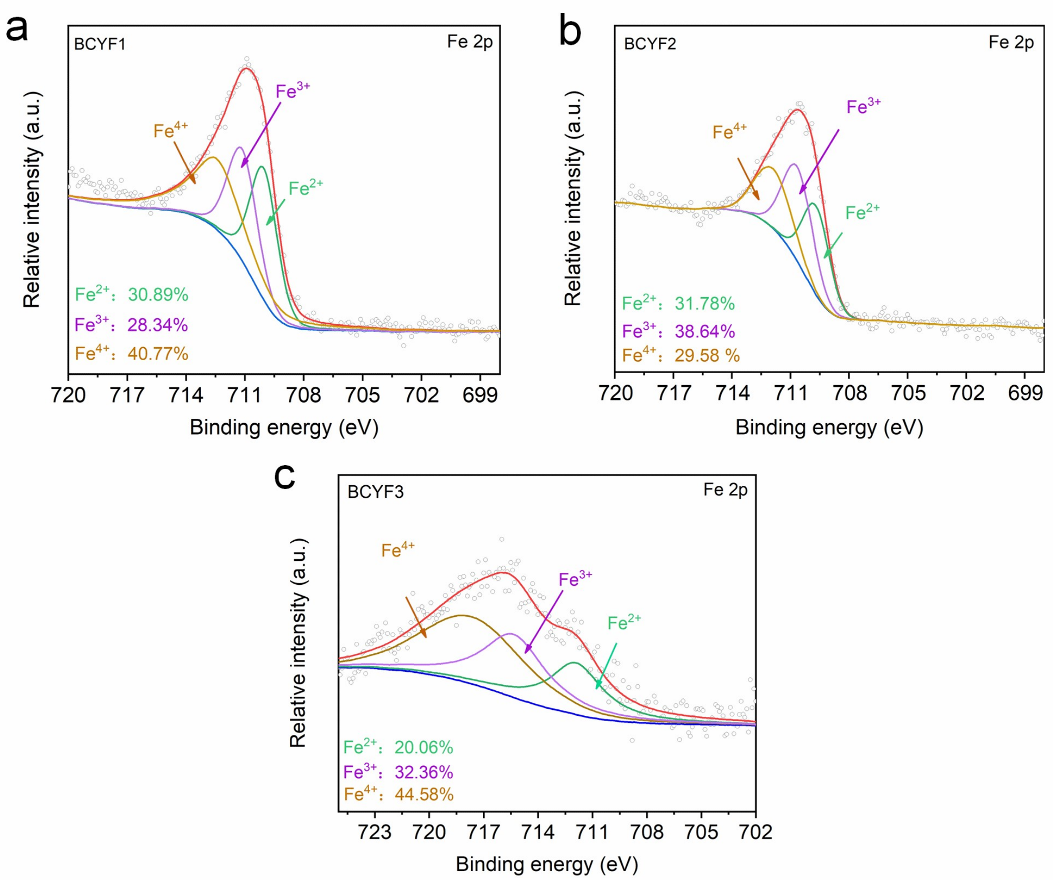

Fig. S9. Fe 2p XPS spectra of (a) BCYF1, (b) BCYF2 and (c) BCYF3 samples.

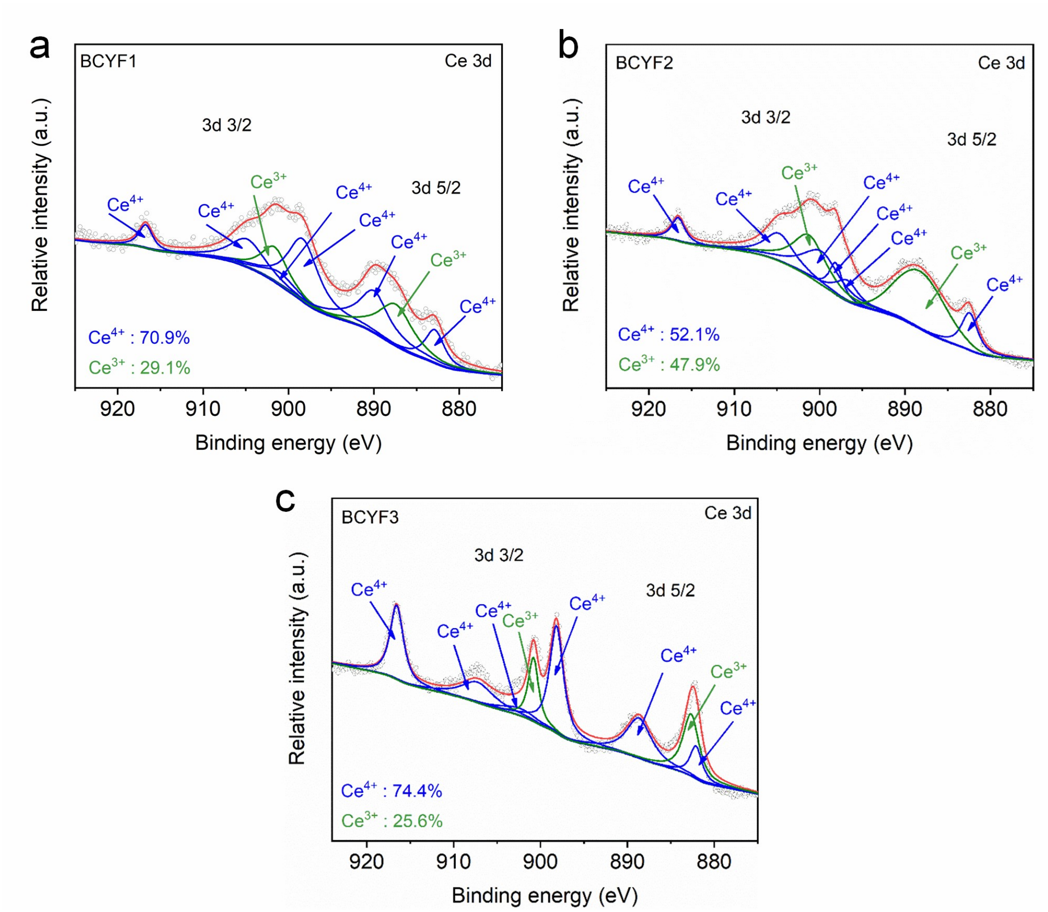

Fig. S10. Ce 3d XPS spectra of (a) BCYF1, (b) BCYF2 and (c) BCYF3 samples.

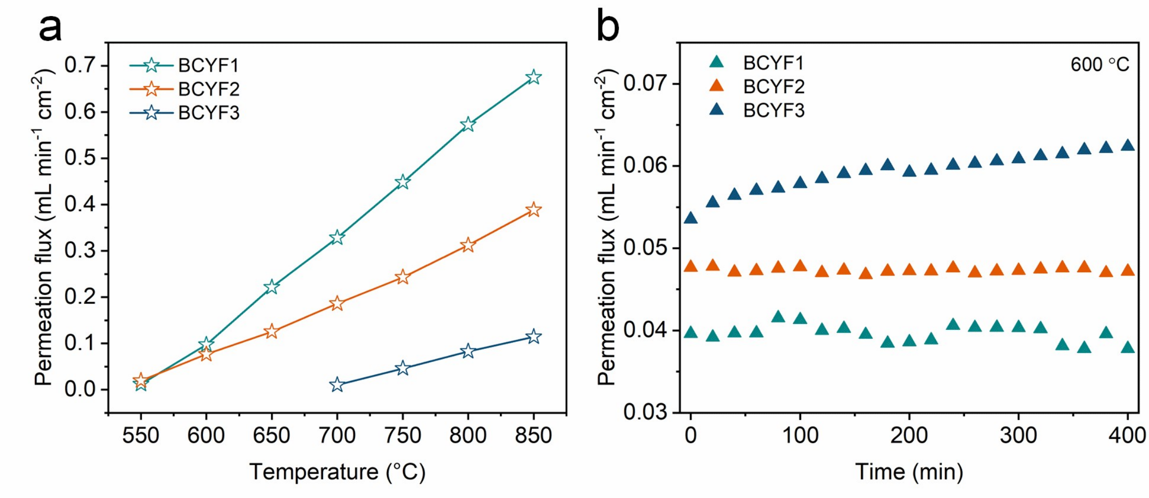

Fig. S11. (a) O_2 permeation rates and (b) H_2 permeation rates of BCYF1, BCYF2 and BCYF3.

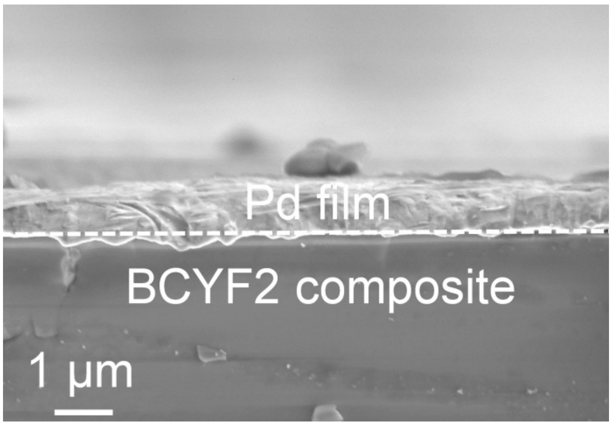

Fig. S12. The typical cross-sectional SEM image of Pd film on the BCYF2 pellet surface.

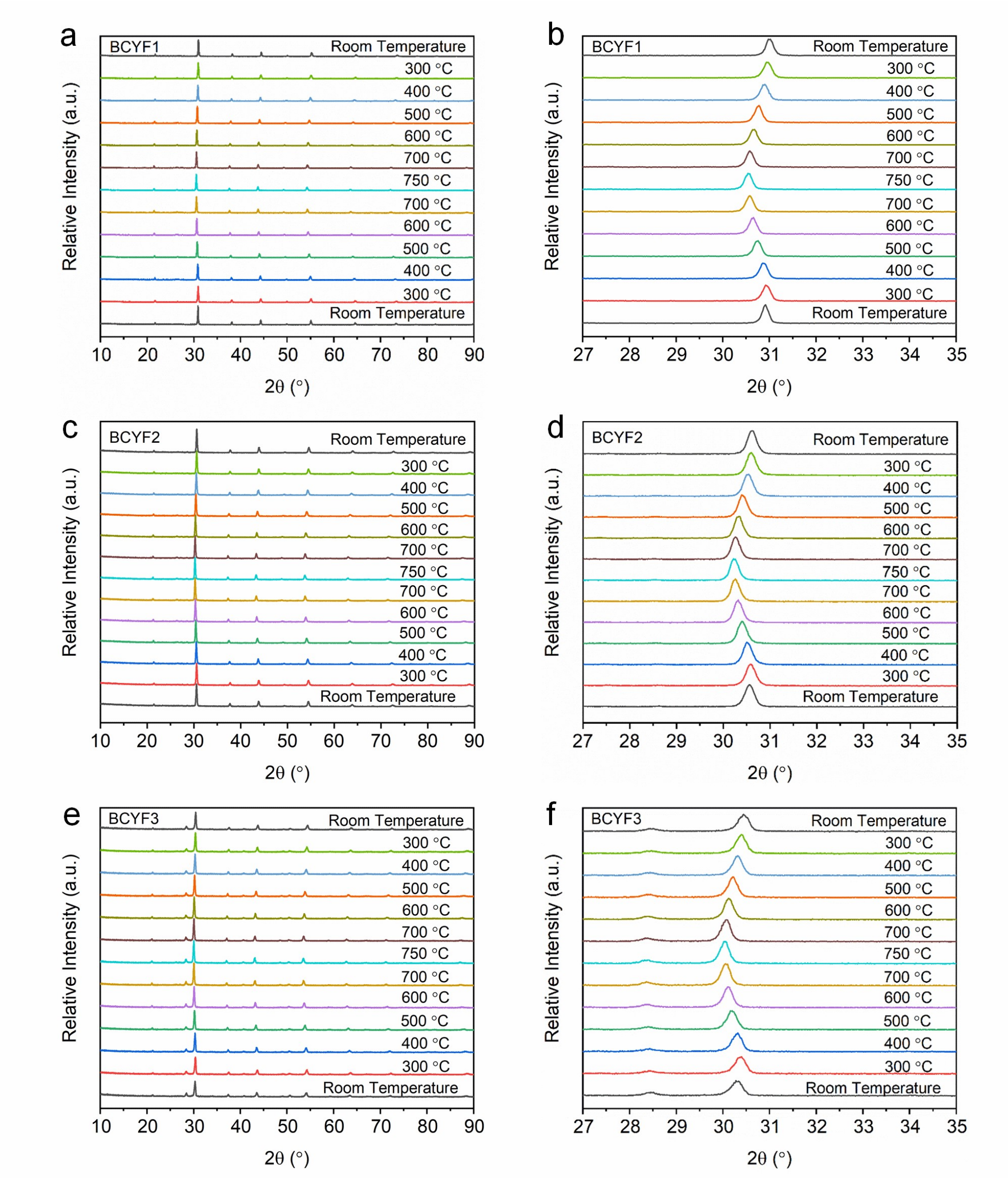

Fig. S13. High-temperature XRD patterns of (a, b) BCYF1, (c, d) BCYF2 and (e, f) BCYF3 sample from room temperature to 750 °C with different 2-theta ranges.

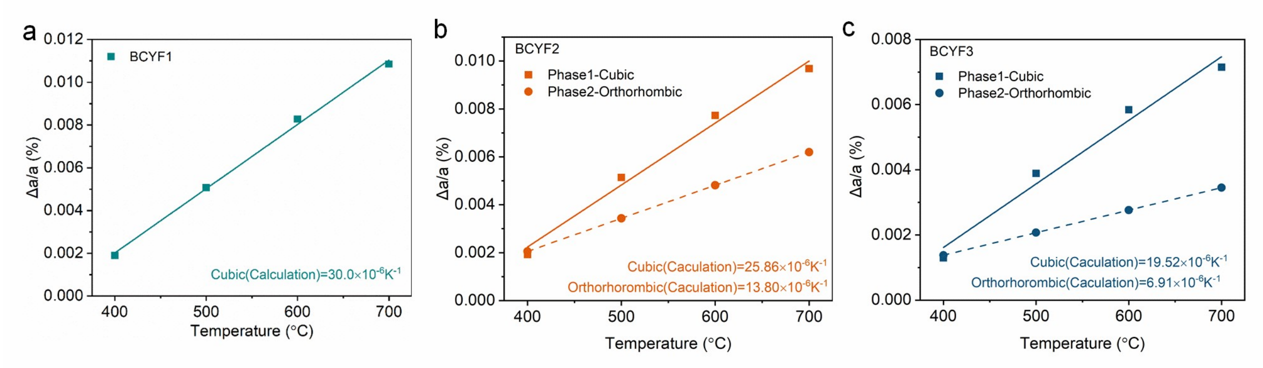

Fig. S14. The calculated TECs of BCYF1, (b) BCYF2 and (c) BCYF3 samples based on HT-XRD patterns.

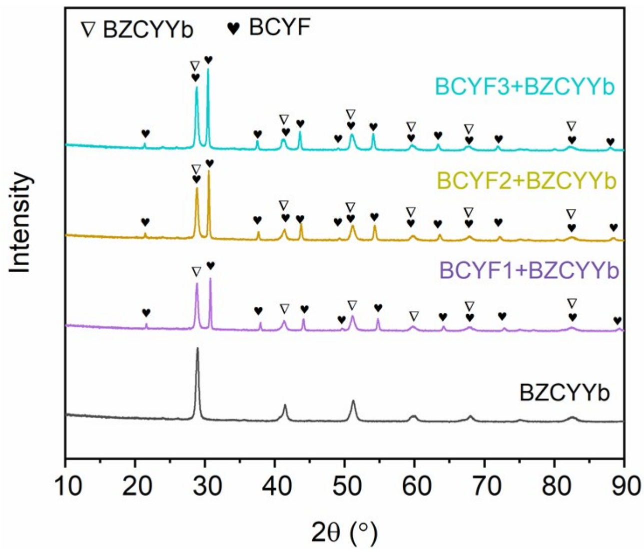

Fig. S15. XRD patterns of BZCYYb and the BCYF+BZCYYb composites (1:1, weight ratio) prepared by physical mixing after a calcination at 1000 °C for 2 h in air.

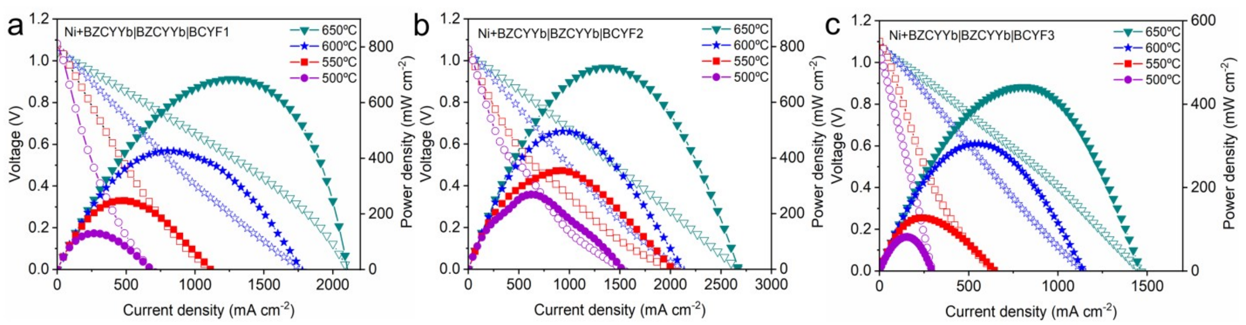

Fig. S16. *I-V* and *I-P* curves of anode-supported single cells with (a) BCYF1, (b) BCYF2 and (c) BCYF3 cathode exposed to static air.

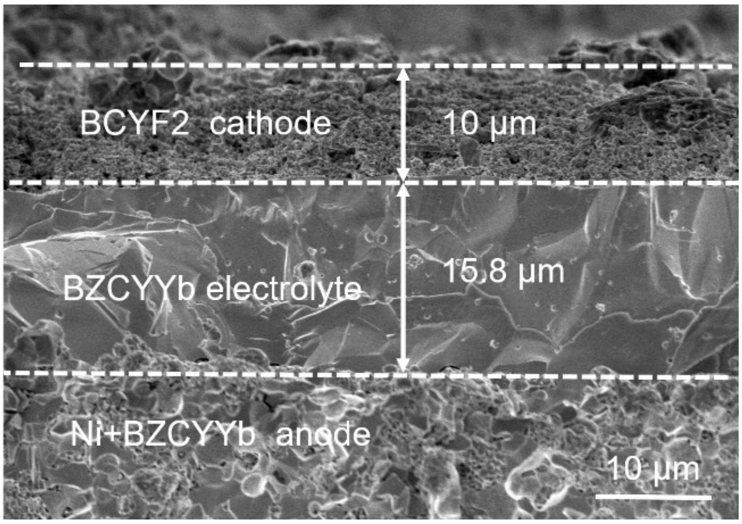

Fig. S17. Cross-sectional SEM image of the anode-supported single cell with BCYF2 cathode.

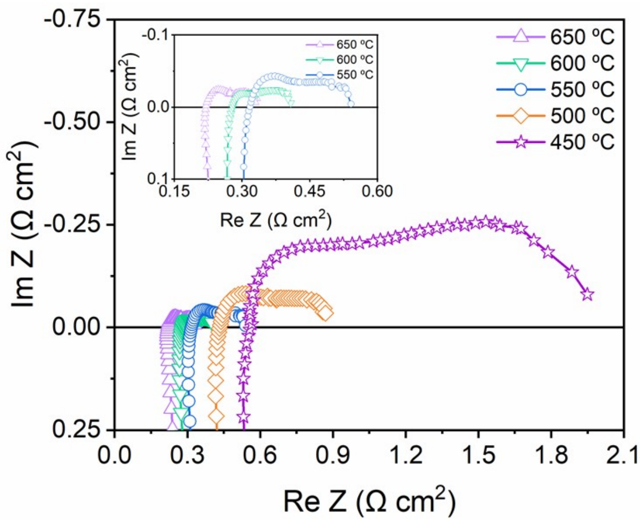

Fig. S18. EIS spectra of the single cell with BCYF2 cathode exposed to flowing air at 650-450 °C.

Table S1. Summary of Rieltveld refinements results for BCYF1, BCYF2 and BCYF3 samples.

Sample	Crystal parameters		Phase proportions (wt. %)	Refinement parameters
BCYF1	Cubic (Pm-3m)	a= 4.0934(3) b=4.0934(3) c=4.0934(3)	100	R_{wp} = 4.99, R_p = 3.70, GOF = 2.03
BCYF2	Cubic (Pm-3m)	a=4.1250(2) b=4.1250(2) c=4.1250(2)	96.6	R_{wp} =5.16, R_p =3.85, GOF = 2.08
	Orthorhombic (Pmcn)	a= 8.7033(6) b=6.2060(0) c=6.2308(0)	3.4	
BCYF3	Cubic (Pm-3m)	a=4.1553(5) b=4.1553(5) c=4.1553(5)	77.0	R_{wp} = 5.65, R_p = 4.13, GOF = 2.34
	Orthorhombic (Pmcn)	a=8.7600(0) b=6.2703(0) c= 6.2083(7)	23.0	

Table S2. Point EDX scanning results of BCYF2 sample.

Element	Atomic ratios at different points (%)									
	1	2	3	4	5	6	7	8	9	10
Ba	35.2	36.8	35	39.8	36.3	33.5	37.5	34.6	35.2	36.0
Fe	6.0	9.1	3.5	18.4	17.7	19.4	17.6	20.9	19.2	20.3
Ce	27.4	22.3	29.2	6.4	4.9	5.5	4.9	5.1	5.2	5.2
Y	1.8	1.4	1.4	1.4	1.6	1.4	1.1	1.2	1.3	1.3
O	29.5	30.4	30.8	33.9	39.4	40.2	38.9	38.1	39.0	37.2

Table S3. ASR values of BCYF1, BCYF2 and BCYF3 cathodes based on SDC electrolyte.

Cathode	Atmosphere	ASR, Ω cm^2 (Temp. °C)				
		650	600	550	500	450
BCYF1	air	0.045	0.090	0.21	0.646	2.72
BCYF2	air	0.05	0.097	0.25	0.594	2.13
BCYF3	air	0.14	0.3	0.63	1.49	4.95

Table S4. ASR value comparison of BCYF2 cathode with other reported Co-free cathodes in O-SOFCs.

Cathode	Electrolyte	ASR, Ω cm^2 (Temp. °C)						Ref.
		750	700	650	600	550	500	
$Ba_{0.5}Sr_{0.5}Fe_{0.8}Cu_{0.2}O_{3-\delta}$ (BSFC)	SDC	/	0.137	0.22	0.365	0.939	/	[1]
$Ba_{0.95}La_{0.05}FeO_{3-\delta}$ (BLF)	SDC	0.021	0.037	0.086	/	/	/	[2]
$BaNb_{0.05}Fe_{0.95}O_{3-\delta}$ (BNF)	SDC	0.016	0.026	0.058	0.147	0.427	/	[3]
$Ba_{0.5}Sr_{0.5}Fe_{0.8}Cu_{0.1}Ti_{0.1}O_{3-\delta}$ (BSFCuTi)	GDC	0.059	0.103	0.19	0.47	/	/	[4]
$BaFe_{0.85}Cu_{0.15}O_{3-\delta}$ (BFC)	CGO	0.35	0.80	2.05	/	/	/	[5]
$BaFe_{0.95}Sn_{0.05}O_{3-\delta}$ (BFS)	SDC	0.018	0.033	0.077	0.207	0.65	/	[6]
$BaFe_{0.75}Ni_{0.25}O_{3-\delta}$ (BFNi25)	CGO	/	0.095	0.184	0.364	/	/	[7]
$Ba_{0.95}Ca_{0.05}Fe_{0.95}In_{0.05}O_{3-\delta}$ (BCFI)	SDC	/	0.038	0.089	0.21	0.44	1.00	[8]
$Sr_{0.9}Ce_{0.1}Fe_{0.8}Ni_{0.2}O_{3-\delta}$ (SCFN)	SDC	/	/	0.028	0.072	0.29	1.28	[9]
BCYF2	**SDC**	**/**	**/**	**0.05**	**0.097**	**0.25**	**0.594**	**This work**

SDC: $Sm_{0.2}Ce_{0.8}O_{1.9}$; GDC: $Gd_{0.2}Ce_{0.8}O_{1.9}$; CGO: $Ce_{0.9}Gd_{0.1}O_{1.95}$

Table S5. ASR values of BCYF1, BCYF2 and BCYF3 cathodes based on BZCYYb electrolyte.

Cathode	Atmosphere	ASR, Ω cm^2 (Temp. °C)				
		650	600	550	500	450
BCYF1	air	0.25	0.49	1.10	2.47	7.16
	5 vol.% H_2O-air	0.20	0.43	0.77	2.38	6.24
BCYF2	air	0.23	0.51	1.13	2.59	6.64
	5 vol.% H_2O-Air	0.16	0.27	0.58	1.49	4.86
BCYF3	air	0.31	0.78	1.99	5.59	14.8
	5 vol.% H_2O-air	0.28	0.55	1.22	2.99	9.05

Table S6. ASR value comparison of BCYF2 cathode with other reported Co-free cathodes in PCFCs.

Cathode	Electrolyte	ASR, Ω cm^2 (Temp. °C)						Atmosphere	Ref.
		750	700	650	600	550	500		
$Ba_{0.95}La_{0.05}Fe_{0.8}Zn_{0.2}O_{3-\delta}$ (BLFZ)	BZCYYb[1]	0.29	0.42	0.66	1.34	/	/	3%H_2O-air	[10]
$Nd_{0.6}Ba_{0.4}Fe_{0.9}Cu_{0.1}O_{3-\delta}$ (NBFC)	BZCYYb[2]	/	/	0.62	1.27	3.99	13.2	3%H_2O-air	[11]
$PrNi_{0.5}Mn_{0.5}O_3$ (PNM)-PrO_x	BZCYYb[1]	0.021	0.052	0.11	0.31	/	/	3%H_2O	[12]
$BaCe_{0.4}Sm_{0.2}Fe_{0.4}O_{3-\delta}$ (BCSF)	BCS	0.24	0.45	0.83	2.02	5.34	/	3%H_2O-air	[13]
$PrBaFe_2O_{5+\delta}$ (PBF)	BZCY	/	0.35	0.70	1.80	/	/	3%H_2O-air	[14]
$Nd_{1.95}Ba_{0.05}NiO_{4+\delta}$ (NBN)	BCZD		6.7	11.6	27.9	69.2		3%H_2O-air	[15]
$Sr_3Fe_2O_{7-\delta}$	BZCY		0.31	0.80	2.41	7.26	26.0	5%H_2O-air	[16]
SCFN	BZCYYb[1]	/	/	0.094	0.23	0.63	2.09	6%H_2O-air	[17]
BCYF2	**BZCYYb[1]**	**/**	**/**	**0.16**	**0.27**	**0.58**	**1.49**	**5%H_2O-air**	**This work**

BZCYYb[1]: $BaZr_{0.1}Ce_{0.7}Y_{0.1}Yb_{0.1}O_{3-\delta}$; BZCYYb[2]: $BaCe_{0.5}Zr_{0.3}Y_{0.1}Yb_{0.1}O_{3-\delta}$; BCS: $BaCe_{0.8}Sm_{0.2}O_{3-\delta}$; BZCY[2]: $BaZr_{0.3}Ce_{0.5}Y_{0.2}O_{3-\delta}$; BCZD: $BaCe_{0.5}Zr_{0.3}Dy_{0.2}O_{3-\delta}$.

Table S7. Peak deconvolution results of XPS spectra for BCYF1, BCYF2 and BCYF3 cathodes

Sample	Fe 2p (%)			Ce 3d (%)		O 1s (%)		
	Fe^{2+}	Fe^{3+}	Fe^{4+}	Ce^{4+}	Ce^{3+}	O_{ads}	O_{lat}	O_{ads}/O_{lat}
BCYF1	30.9	28.3	40.8	70.9	29.1	86.6	13.4	6.46
BCYF2	31.8	38.6	29.6	52.1	47.9	85.8	14.2	6.04
BCYF3	20.0	32.4	44.6	74.4	25.6	41.7	58.3	0.71

Table S8. Evolution of ASR values of BCYF1, BCYF2 and BCYF3 in BZCYYb-based symmetrical cells in 5 vol.% H_2O-air (with and without 1 vol.% CO_2) at 600 °C.

Cathode	ASR (Ω cm^2) against the exposure time (min)									
	5 vol.%H_2O-air+1 vol.% CO_2						after the CO_2 removal			
	0	20	40	60	80	100	120	140	160	180
BCYF1	0.35	0.75	0.60	0.68	0.76	0.64	0.43	0.47	0.52	0.46
BCYF2	0.21	0.64	0.65	0.67	0.69	0.69	0.16	0.19	0.17	0.18
BCYF3	0.70	2.78	2.94	3.06	3.08	3.35	0.82	0.83	0.81	0.78

Table S9. PPD value comparison of PCFCs based on BCYF2 cathode and other reported Co-free cathodes.

Cathode	Electrolyte	PPD at 600 °C (mW cm^{-2})	Ref.
$BaCe_{0.5}Fe_{0.5}O_{3-\delta}$	$BaZr_{0.1}Ce_{0.7}Y_{0.2}O_{3-\delta}$	192	[18]
$Ba_{0.95}La_{0.05}Fe_{0.8}Zn_{0.2}O_{3-\delta}$-$BaZr_{0.1}Ce_{0.7}Y_{0.1}Yb_{0.1}O_{3-\delta}$	$BaZr_{0.1}Ce_{0.7}Y_{0.1}Yb_{0.1}O_{3-\delta}$	142	[10]
$BaCe_{0.5}Fe_{0.3}Bi_{0.2}O_{3-\delta}$	$BaZr_{0.1}Ce_{0.7}Y_{0.2}O_{3-\delta}$	362	[19]
$BaFe_{0.8}Ce_{0.1}Y_{0.1}O_{3-\delta}$-$BaCe_{0.8}Fe_{0.1}Y_{0.1}O_{3-\delta}$	$BaZr_{0.1}Ce_{0.7}Y_{0.2}O_{3-\delta}$	417	[20]
$BaCe_{0.1}Zr_{0.2}Y_{0.1}Fe_{0.6}O_{3-\delta}$	$BaCe_{0.5}Zr_{0.3}Y_{0.1}Yb_{0.1}O_{3-\delta}$	74	[21]
$BaZr_{0.2}Fe_{0.6}Y_{0.2}O_{3-\delta}$	$BaZr_{0.1}Ce_{0.7}Y_{0.2}O_{3-\delta}$	175	[22]
$La_{0.35}Pr_{0.15}Sr_{0.5}FeO_{3-\delta}$	$BaZr_{0.1}Ce_{0.7}Y_{0.2}O_{3-\delta}$	400	[23]
$BaFe_{0.5}Sn_{0.2}Bi_{0.3}O_{3-\delta}$	$BaZr_{0.1}Ce_{0.7}Y_{0.2}O_{3-\delta}$	841	[24]
$Bi_{0.5}Ba_{0.5}FeO_{3-\delta}$	$BaZr_{0.1}Ce_{0.7}Y_{0.2}O_{3-\delta}$	38	[25]
$Ca_{0.3}Y_{0.7}Fe_{0.5}Co_{0.5}O_{3-\delta}$- $BaZr_{0.1}Ce_{0.7}Y_{0.2}O_{3-\delta}$	$BaZr_{0.1}Ce_{0.7}Y_{0.2}O_{3-\delta}$	300	[26]
$Ba_{0.95}Ca_{0.05}Fe_{0.85}Sn_{0.05}Y_{0.1}O_{2.9-\delta}F_{0.1}$- $Ce_{0.8}Sm_{0.2}O_{2-\delta}$	$BaZr_{0.1}Ce_{0.7}Y_{0.2}O_{3-\delta}$	641	[27]
$Sr_3Fe_2O_{7-\delta}$- $BaZr_{0.3}Ce_{0.5}Y_{0.2}O_{3-\delta}$	$BaZr_{0.3}Ce_{0.5}Y_{0.2}O_{3-\delta}$	380	[16]
$BaCe_{0.2}Fe_{0.6}Pr_{0.2}O_{3-\delta}$	$BaZr_{0.1}Ce_{0.7}Y_{0.2}O_{3-\delta}$	316	[28]
$Pr_2BaNiMnO_{3-\delta}$	$BaZr_{0.1}Ce_{0.7}Y_{0.1}Yb_{0.1}O_{3-\delta}$	570	[29]
$Ba_{0.5}Sr_{0.5}Zn_{0.2}Fe_{0.8}O_{3-\delta}$	$BaZr_{0.1}Ce_{0.7}Y_{0.2}O_{3-\delta}$	277	[30]
BCYF2	$\mathbf{BaZr_{0.1}Ce_{0.7}Y_{0.1}Yb_{0.1}O_{3-\delta}}$	**656**	**This work**

References

[1] L. Zhao, B. He, X. Zhang, R. Peng, G. Meng and X. Liu, *J. Power Sources*, 2010, **195**, 1859-1861.

[2] F. Dong, D. Chen, Y. Chen, Q. Zhao and Z. Shao, *J. Mater. Chem.*, 2012, **22**, 15071-15079.

[3] F. Dong, Y. Chen, R. Ran, D. Chen, M.O. Tadé, S. Liu and Z. Shao, *J. Mater. Chem. A*, 2013, **1**, 9781-9791.

[4] G. Yang, J. Shen, Y. Chen, O. Tadé and Z. Shao, *J. Power Sources*, 2015, **298**, 184-192.

[5] M. Zhu, Z. Cai, T. Xia, Q. Li, L. Huo and H. Zhao, *Int. J. Hydrogen Energy*, 2016, **41**, 4784-4791.

[6] F. Dong, M. Ni, W. He, Y. Chen, G. Yang, D. Chen and Z. Shao, *J. Power Sources*, 2016, **326**, 459-465.

[7] L. Gao, M. Zhu, T. Xia, Q. Li, T. Li and H. Zhao, *Electrochim. Acta*, 2018, **289**, 428-436.

[8] J. Wang, Y. Lam, M. Saccoccio, Y. Gao, D. Chen and F. Ciucci, *J. Power Sources*, 2016, **324**, 224-232.

[9] Y. Song, Y. Chen, M. Xu, W. Wang, Y. Zhang, G. Yang, R. Ran, W. Zhou and Z. Shao, *Adv. Mater.*, 2020, **32**, 1906979.

[10] Z. Wang, P. Lv, L. Yang, R. Guan, J. Jiang, F. Jin and T. He, *Ceram. Int.*, 2020, **46**, 18216-18223.

[11] R. Tarutina, G. Lyagaeva, S. Farlenkov, I. Vylkov, K. Vdovin, A. Murashkina, K. Demin and A. Medvedev, *J. Solid State Electrochem.*, 2020, **24**, 1453-1462.

[12] Y. Chen, S. Yoo, K. Pei, D. Chen, L. Zhang and B. deGlee, *Adv. Funct. Mater.*, 2017, **28**, 1704907.

[13] C. Zhang and H. Zhao, *J. Mater. Chem.*, 2012, **22**, 18387-18394.

[14] D. Kim, J. Son, M. Kim, J. Park and H. Joo, *J. Eur. Ceram. Soc.*, 2021, **41**, 5939-5946.

[15] N. Danilov, J. Lyagaeva, G. Vdovin, E. Pikalova and D. Medvedev, *Energy Convers. Manage.*, 2018, **172**, 129-137.

[16] Z. Wang, W. Yang, P. Shafi, L. Bi, Z. Wang, R. Peng, C. Xia, W. Liu and Y. Lu, *J. Mater. Chem. A*, 2015, **3**, 8405-8412.

[17] Y. Song, J. Liu, Y. Wang, D. Guan, A. Seong, M. Liang, M. J. Robson, X. Xiong, Z. Zhang, G. Kim, Z. Shao and F. Ciucci, *Adv. Energy Mater.* 2021, **11**, 2101899.

[18] Z. Tao, L. Bi, Z. Zhu and W. Liu, *J. Power Sources*, 2009, **194**, 801-804.

[19] D. Shan, Z. Gong, Y. Wu, L. Miao, K. Dong and W. Liu, *Ceram. Int.*, 2017, **43**, 3660-3663.

[20] Z. Wei, J. Wang, X. Yu, Z. Li, Y. Zhao and J. Chai, *Int. J. Hydrogen Energy*, 2021, **46**, 23868-23878.

[21] R. Tarutina, K. Vdovin, G. Lyagaeva and A. Medvedev, J. Alloys Compd., 2020, 831, 154895.

[22] Y. Wu, K. Li, Y. Yang, W. Song, Z. Ma, H. Chen, X. Ou, L. Zhao, M. Khan and Y. Ling, J.

Alloys Compd., 2020, 814, 152220.

[23] X. Xu, H. Wang, J. Ma, W. Liu, X. Wang, M. Fronzi and L. Bi, *J. Mater. Chem. A*, 2019, **7**, 18792-18798.

[24] Y. Xia, Z. Jin, H. Wang, Z. Gong, H. Lv, R. Peng, W. Liu and L. Bi, *J. Mater. Chem. A*, 2019, **7**, 16136-16148.

[25] J. Cui, J. Wang, X. Zhang, G. Li, K. Wu, Y. Cheng and J. Zhou, *Int. J. Hydrogen Energy*, 2019, **44**, 21127-21135.

[26] J. Cui, J. Wang, X. Zhang, G. Li, K. Wu, Y. Cheng and J. Zhou, *J. Power Sources*, 2019, **413**, 148-157.

[27] J. Liu, Z. Jin, L. Miao, J. Ding, H. Tang, Z. Gong, R. Peng and W. Liu, *Int. J. Hydrogen Energy*, 2019, **44**, 11079-11087.

[28] X. Zhou, N. Hou, T. Gan, L. Fan, Y. Zhang, J. Li, G. Gao, Y. Zhao and Y. Li, *J. Power Sources*, 2021, **495**, 229776.

[29] Q. Wang, J. Hou, Y. Fan, X. Xi, J. Li, Y. Lu, G. Huo, L. Shao, Z. Fu and L. Luo, *J. Mater. Chem. A*, 2020, **8**, 7704-7712.

[30] H. Ding, B. Lin, X. Liu and G. Meng, *Electrochem. Commun.*, 2008, **10**, 1388-1391.